

# Double-strand DNA cleavage by copper complexes of 2,2'-dipyridyl with electropositive pendants†

Yan An, Ming-Liang Tong, Liang-Nian Ji and Zong-Wan Mao\*

Received 14th November 2005, Accepted 24th January 2006

First published as an Advance Article on the web 31st January 2006

DOI: 10.1039/b516132k

Two highly charged cationic copper(II) complexes have been synthesized and characterized structurally and spectroscopically:  $[\text{Cu}(\text{L}^1)_2(\text{Br})](\text{ClO}_4)_5$  (**1**) and  $[\text{Cu}(\text{L}^2)_2(\text{Br})](\text{ClO}_4)_5$  (**2**) ( $\text{L}^1 = 5,5'$ -di(1-(triethylammonio)methyl)-2,2'-dipyridyl cation and  $\text{L}^2 = 5,5'$ -di(1-(tributylammonio)methyl)-2,2'-dipyridyl cation bidentate ligands). X-Ray structures show that Cu(II) ions in both complexes have a trigonal-bipyramidal  $\text{CuN}_4\text{Br}$ -configuration. Two nitrogen atoms of the electropositive pendants and coordinated bromine atom basically array in a straight line. Their close distances of  $\text{N}\cdots\text{Br}$  atoms are 5.772 and 5.594 Å, respectively, which is comparable to that of adjacent phosphodiester in B-form DNA (*ca.* 6 Å). In the absence of reducing agent, supercoiled plasmid DNA cleavage by the complexes has been performed and their hydrolytic mechanisms have been investigated. The pseudo-Michaelis–Menten kinetic parameters ( $k_{\text{cat}}$ ), 4.15  $\text{h}^{-1}$  for **1**, 0.43  $\text{h}^{-1}$  for **2** and 0.61  $\text{h}^{-1}$  for  $[\text{Cu}(\text{bipy})(\text{NO}_3)_2]$ , were obtained. This result indicates that **1** exhibits markedly higher nuclease activity than its corresponding analogues. The high ability of DNA cleavage for **1** is attributed to the effective cooperation of the metal moiety and two positive pendants since the array of linear tri-binding sites matches with one of three phosphodiester backbones of nucleic acid.

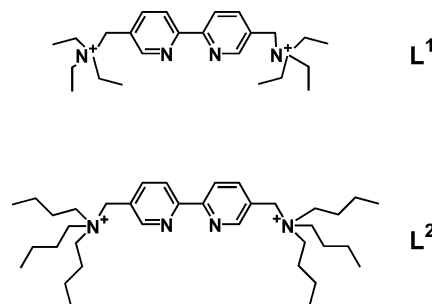
## Introduction

Transition metal complexes that cleave DNA under physiological condition are of current interest in the development of artificial nucleases.<sup>1–10</sup> Morrow *et al.* reported detailed kinetic studies on the transesterification of the 2-(4-nitrophenyl phosphate) ester of propylene glycol promoted by various metal ions and found the ability of metal ions to promote the transesterification followed the order  $\text{Cu}^{2+} > \text{Zn}^{2+} \gg \text{Co}^{2+} > \text{Mn}^{2+} > \text{Ni}^{2+}$ .<sup>11</sup> Subsequently, many Cu(II) complexes, including mononuclear,<sup>12–23</sup> dinuclear,<sup>24–32</sup> trinuclear,<sup>33–37</sup> and even macromolecular catalytic systems,<sup>38,39</sup> have been applied as catalysts for efficient cleavage of nucleic acids in the absence of or in the presence of a reducing agent. In view of a number of nucleases having two or more than two metal ions in the catalytic centre,<sup>40</sup> considerable effort has been made to develop multi-metal models.<sup>24–39</sup> Of those reported, however, the most highly efficient cleavage agents involving hydrolytic mechanism are three mononuclear Cu(II) complexes: a Cu–dpq complex with a rate constant of 5.58  $\text{h}^{-1}$  (pH = 7.2),<sup>12a</sup> a Cu–tach complex with a rate constant of 4.34  $\text{h}^{-1}$  (pH = 8.1)<sup>22</sup> and a Cu–neamin complex with a rate constant of 3.57  $\text{h}^{-1}$  (pH = 7.3).<sup>19</sup> In the latter, the sugars play an important role in interaction between the complex and DNA.

Kramer and co-workers reported that a copper-binding bipy unit with 3,3'-ammonium groups can increase the hydrolytic rate of phosphate diesters.<sup>41</sup> Furthermore, peralkylated ammo-

nium groups were chosen instead of free amines, results in formation of rather stable phosphoramides. A previous report shows that peralkylammoniums have approximately the same affinity for DNA as the corresponding protonated polyamines.<sup>42</sup> The introduction of positive charges in the side chains of the ligands may open a way to activate the phosphates to ease the liberation of leaving phosphate anion and, in particular, to stabilize pretransition state complexes with nucleotides and with double-stranded (ds) DNA.

Therefore, one of approaches is to construct bifunctional models promoting phosphodiester hydrolysis through cooperation of metal ions and functional groups. To mimic efficient nuclease models, two bipy-based ligands with doubly electropositive pendants (Scheme 1), 5,5'-di[1-(triethylammonio)methyl]-2,2'-dipyridyl ( $\text{L}^1$ ) and 5,5'-di[1-(tributylammonio)methyl]-2,2'-dipyridyl ( $\text{L}^2$ ), and their Cu(II) complexes were designed and synthesized according to a linear DNA strand. In this paper, we present the synthesis and X-ray crystal structures of Cu(II) complexes and interaction and cleavage to DNA.



Scheme 1 Schematic illustration of ligands  $\text{L}^1$  and  $\text{L}^2$ .

School of Chemistry and Chemical Engineering, Sun Yat-Sen University, Guangzhou, 510275, China. E-mail: cesmzw@zsu.edu.cn; Fax: (+86) 20 84112245

† Electronic supplementary information (ESI) available:  $^1\text{H}$  NMR and MS spectra of the ligands, the  $T_m$  curves of DNA, the agarose gel electrophoresis and corresponding time course of DNA cleavage by the complexes. See DOI: 10.1039/b516132k

## Experimental

### Materials

5,5'-Dimethyl-2,2'-dipyridyl was purchased from Aldrich Chemical Co. The pBR322 DNA was purchased from MBI. Catalase was purchased from BBI. Ethidium bromide and HEPES were purchased from AMRESCO. Other reagents of analytical grade were obtained from commercial suppliers and used directly without further purification. Milli-Q water was used in all physical measurement experiments.

### Preparation of ligands and complexes

**CAUTION:** although no problems were encountered in this work, transition-metal perchlorates are potentially explosive and should thus be prepared in small quantities and handled with care.

**5,5'-Dibromomethyl-2,2'-dipyridyl.** A mixture of 5,5'-dimethyl-2,2'-dipyridyl (5.53 g, 30.0 mmol), *N*-bromosuccinimide (10.7 g, 60.0 mmol) in tetrachloromethane (300 mL) were stirred for 0.5 h at 80 °C. Benzoyl peroxide (60.0 mg) was added to the mixture and continued to be stirred for 2 h. The hot mixture was then filtered and the filtrate was evaporated under reduced pressure to remove tetrachloromethane. A pale yellow solid was formed and recrystallized from tetrahydrofuran to yield a white powder (3.02 g, 29.4%), mp 192.7–193.0 °C. Elemental analysis data: calc. (%) for C<sub>12</sub>H<sub>10</sub>Br<sub>2</sub>N<sub>2</sub> (342.03): C 42.14, H 2.95, N 8.19; found: C 41.93, H 3.24, N 8.22.

**5,5'-Di[1-(triethylammonio)methyl]-2,2'-dipyridyl bromide tetrahydrate (L<sup>1</sup>Br<sub>2</sub>·4H<sub>2</sub>O).** 5,5'-Dibromomethyl-2,2'-dipyridyl (0.342 g, 1.00 mmol) and triethylamine (0.364 g, 3.60 mmol) were mixed in 32.0 mL of dry chloroform in room temperature for 5 h. The solution was then filtered and the resulted white powder was washed with chloroform and dried in vacuum (0.397 g, 72.9%). Elemental analysis data: calc. (%) for C<sub>24</sub>H<sub>40</sub>Br<sub>2</sub>N<sub>4</sub>·4H<sub>2</sub>O (616.48): C 46.76, H 7.85, N 9.09; found: C 46.69, H 7.32, N 9.01; ESI-MS: *m/z* (%): 192.2 (100) [L<sup>1</sup>]<sup>2+</sup>; <sup>1</sup>H NMR (D<sub>2</sub>O, 300 MHz): δ 8.833 (s, 2H, PyH), 8.343 (d, 2H, PyH), 8.221 (d, 2H, PyH), 4.654 (s, 4H, NCH<sub>2</sub>Py), 3.410 (m, 12H, NCH<sub>2</sub>Me), 1.526 (t, 18H, CH<sub>3</sub>).

**5,5'-Di[1-(tributylammonio)methyl]-2,2'-dipyridyl bromide (L<sup>2</sup>Br<sub>2</sub>).** 5,5'-Dibromomethyl-2,2'-dipyridyl (0.342 g, 1.00 mmol) and tributylamine (0.667 g, 3.60 mmol) were mixed in 32 mL of dry chloroform in room temperature. The mixture was kept under Ar atmosphere for 48 h. The solution was then filtered and the resulting white powder was washed with chloroform and dried in vacuum (0.439 g, 61.6%). Elemental analysis data: calc. (%) for C<sub>36</sub>H<sub>60</sub>Br<sub>2</sub>N<sub>4</sub> (712.74): C 60.67, H 9.05, N 7.86; found: C 60.71, H 9.02, N 7.87; ESI-MS: *m/z* (%): 276.3 (100) [L<sup>2</sup>]<sup>2+</sup>; <sup>1</sup>H NMR (DMSO-*d*<sub>6</sub>, 300 MHz): δ 8.792 (s, 2H, PyH), 8.336–8.308 (d, 2H, PyH), 8.189–8.155 (d, 2H, PyH), 4.683 (s, 4H, NCH<sub>2</sub>Py), 3.297–3.242 (t, 12H, NCH<sub>2</sub>Pr), 1.894–1.843 (m, 12H, NMeCH<sub>2</sub>Et), 1.481–1.386 (m, 12H, NEtCH<sub>2</sub>Me), 1.044–0.996 (t, 18H, CH<sub>3</sub>).

**[Cu(L<sup>1</sup>)<sub>2</sub>(Br)](ClO<sub>4</sub>)<sub>5</sub>·6H<sub>2</sub>O (1).** A methanol solution of Cu(ClO<sub>4</sub>)<sub>2</sub>·6H<sub>2</sub>O (0.074 g, 0.198 mmol) was added to a solution of L<sup>1</sup>Br<sub>2</sub>·4H<sub>2</sub>O (0.123 g, 0.199 mmol) in 3 mL of methanol and brown powder was obtained. The powder was recrystallized from hot water. Several days later, green crystals were collected and dried

(0.050 g, 32.9%). Obtained crystals are suitable for X-ray analysis. Elemental analysis data: calc. (%) for C<sub>48</sub>H<sub>80</sub>BrCl<sub>5</sub>CuN<sub>8</sub>O<sub>20</sub>·6H<sub>2</sub>O (1518.01): C 37.98, H 6.11, N 7.38; found: C 38.09, H 6.16, N 7.19; ESI-MS: *m/z* (%): 483.2 (100) [L<sup>1</sup>(ClO<sub>4</sub>)]<sup>+</sup>, 609.0 (12) [Cu(L<sup>1</sup>)<sub>2</sub>(Br)(ClO<sub>4</sub>)<sub>3</sub>]<sup>2+</sup>.

**[Cu(L<sup>2</sup>)<sub>2</sub>(Br)](ClO<sub>4</sub>)<sub>5</sub> (2).** Cu(ClO<sub>4</sub>)<sub>2</sub>·6H<sub>2</sub>O (0.074 g, 0.198 mmol) was dissolved in ethanol, and an ethanol solution of L<sup>2</sup>Br<sub>2</sub> (0.142 g, 0.199 mmol) was added to the stirred solution. A purple powder was obtained and recrystallized from methanol to obtain green crystals (0.069 g, 39.5%). The obtained crystals are suitable for X-ray analysis. Elemental analysis data: calc. (%) for C<sub>72</sub>H<sub>128</sub>BrCl<sub>5</sub>CuN<sub>8</sub>O<sub>20</sub> (1746.56): C 49.51, H 7.39, N 6.42; found: C 49.34, H 7.33, N 6.46; ESI-MS: *m/z* (%): 1646.13 (100) [Cu(L<sup>2</sup>)<sub>2</sub>Br(ClO<sub>4</sub>)<sub>4</sub>]<sup>+</sup>, 1666.47 (45) [Cu(L<sup>2</sup>)<sub>2</sub>(ClO<sub>4</sub>)<sub>5</sub>]<sup>+</sup>.

### General methods

Microanalyses (C, H and N) were carried out with an Elementar Vario EL elemental analyser. UV-vis spectroscopy was recorded on a Varian Cary 100 spectrophotometer with a thermostatic cell holder and NMR spectroscopy was performed on a Varian Inova 500/Mercury plus 300 NMR spectrometer with D<sub>2</sub>O or DMSO-*d*<sub>6</sub> as a solvent. An LCQ DECA XP electrospray mass spectrometer was employed for the investigation of charged ligands in the mixture of water and methanol.

### X-Ray crystallography

Single crystals of complexes **1** and **2** with approximate dimensions 0.32 × 0.28 × 0.22 mm (**1**), 0.28 × 0.26 × 0.20 mm (**2**) were used for X-ray diffraction analyses. The crystals were mounted on the end of a thin glass fiber using an inert epoxy gel. Data collection of **1** and **2** was performed with Mo-K $\alpha$  radiation ( $\lambda = 0.71073$  Å) on a Bruker Apex CCD diffractometer at 123(2) and 293(2) K for **1** and **2**, respectively. The raw data frames were integrated with SAINT<sup>+</sup>, which also applied corrections for Lorentz and polarization effects. Absorption corrections were applied by using the multiscan program SADABS.<sup>43</sup> The structures were solved by direct methods, and all non-hydrogen atoms were refined anisotropically by least-squares on *F*<sup>2</sup> using the SHELXTL program.<sup>44</sup> Hydrogen atoms on organic ligands were generated by the riding mode (C–H = 0.96 Å); the aqua, hydroxy and ammonia hydrogen atoms were located from difference maps. For **2**, the Flack parameter is –0.019(18). A summary of the crystal data is given in Table 1. Selected bond distances and bond angles are listed in Tables 2 and 3.

CCDC reference numbers 289491 and 289492.

For crystallographic data in CIF or other electronic format see DOI: 10.1039/b516132k

### Thermal melting curves and $\Delta T_m$ calculation

The concentration of the calf thymus (CT) DNA was determined spectrophotometrically on the basis of known molar extinction coefficient ( $\epsilon_{260}$ ) 6600 dm<sup>3</sup> mol<sup>-1</sup> cm<sup>-1</sup>.<sup>20a,45</sup> Thermal melting curves were obtained on a Cary 100 UV-vis spectrophotometer connected to a temperature controller. The melting curves were recorded at different molar ratio of compound to DNA (*r*) by measurement of the changes in absorption at 260 nm as a function of temperature

**Table 1** Crystallographic data for complexes **1** and **2**

Complex	<b>1</b>	<b>2</b>
Empirical formula	C <sub>48</sub> H <sub>98</sub> BrCl <sub>5</sub> CuN <sub>8</sub> O <sub>29</sub>	C <sub>72</sub> H <sub>128</sub> BrCl <sub>5</sub> CuN <sub>8</sub> O <sub>20</sub>
<i>M<sub>r</sub></i>	1572.04	1746.56
<i>T</i> /K	123(2)	273(2)
$\lambda$ /Å	0.71073	0.71073
Crystal system	Monoclinic	Orthorhombic
Space group	<i>P</i> 2 <sub>1</sub> / <i>c</i>	<i>Pna</i> 2 <sub>1</sub>
<i>a</i> /Å	14.2945(11)	17.405(4)
<i>b</i> /Å	14.4469(11)	36.500(9)
<i>c</i> /Å	34.637(3)	14.163(4)
$\beta$ /°	101.088(2)	
<i>V</i> /Å <sup>3</sup>	7019.4(9)	8997(4)
<i>Z</i>	4	4
<i>D<sub>c</sub></i> /g cm <sup>-3</sup>	1.488	1.283
$\mu$ /mm <sup>-1</sup>	1.156	0.902
<i>F</i> (000)	3292	3700
Crystal size/mm	0.32 × 0.28 × 0.22	0.28 × 0.26 × 0.20
$\theta$ Range for data collection/°	1.45–26.00	1.94–25.0
Limiting indices, <i>hkl</i>	–10 to 17, –15 to 17, –41 to 42	–20 to 18, –43 to 42, –16 to 16
Reflections collected	29749	46184
Independent reflections ( <i>R</i> <sub>int</sub> )	13292 (0.0456)	15557 (0.0438)
Goodness-of-fit on <i>F</i> <sup>2</sup>	1.029	1.034
<i>R</i> <sub>1</sub> / <i>wR</i> <sub>2</sub> [ <i>I</i> > 2 $\sigma$ ( <i>I</i> )] <sup>a</sup>	0.0747/0.1851	0.0915/0.2448
<i>R</i> <sub>1</sub> / <i>wR</i> <sub>2</sub> (all data) <sup>a</sup>	0.1078/0.2074	0.1462/0.3021
Largest diff. peak/e Å <sup>-3</sup>	5.064/–0.870	0.855/–1.040

$$^a R_1 = \sum \|F_o\| - |F_c| / \sum \|F_o\|, wR_2 = [\sum w(F_o^2 - F_c^2)^2 / \sum w(F_o^2)^2]^{1/2}.$$

**Table 2** Selected bond lengths (Å) and angles (°) for the metal environment of **1**

Cu(1)–N(1)	1.998(3)	Cu(1)–Br(1)	2.4592(6)
Cu(1)–N(2)	2.074(3)	N(3)···Br(1)	5.772
Cu(1)–N(5)	1.984(3)	N(7)···Br(1)	5.595
Cu(1)–N(6)	2.094(3)		
N(5)–Cu(1)–N(1)	174.1(1)	N(2)–Cu(1)–N(6)	115.1(1)
N(5)–Cu(1)–N(2)	96.0(1)	N(5)–Cu(1)–Br(1)	92.91(9)
N(1)–Cu(1)–N(2)	80.4(1)	N(1)–Cu(1)–Br(1)	93.01(9)
N(5)–Cu(1)–N(6)	79.6(1)	N(2)–Cu(1)–Br(1)	128.97(8)
N(1)–Cu(1)–N(6)	97.6(1)	N(6)–Cu(1)–Br(1)	115.94(8)
N(3)···Br(1)···N(7)	177.7		

**Table 3** Selected bond lengths (Å) and angles (°) for the metal environment of **2**

Cu(1)–N(1)	2.003(5)	Cu(1)–Br(1)	2.406(1)
Cu(1)–N(2)	2.093(5)	N(3)···Br(1)	5.933
Cu(1)–N(5)	2.091(5)	N(8)···Br(1)	5.320
Cu(1)–N(6)	1.992(5)		
N(6)–Cu(1)–N(1)	170.0(2)	N(6)–Cu(1)–Br(1)	95.4(1)
N(6)–Cu(1)–N(5)	79.2(2)	N(1)–Cu(1)–Br(1)	94.2(2)
N(1)–Cu(1)–N(5)	92.6(2)	N(5)–Cu(1)–Br(1)	128.0(1)
N(6)–Cu(1)–N(2)	98.7(2)	N(2)–Cu(1)–Br(1)	120.0(1)
N(1)–Cu(1)–N(2)	79.0(2)	N(3)···Br(1)···N(8)	170.2
N(5)–Cu(1)–N(2)	111.9(2)		

in the range of 55–95 °C. *T<sub>m</sub>* values were determined from the maximum of the first derivative or tangentially from the graph at midpoint of the transition curves.  $\Delta T_m$  values were calculated by subtracting *T<sub>m</sub>* of the free nucleic acid from the *T<sub>m</sub>* of the nucleic acid interacted by the complex.

## DNA cleavage and *k<sub>obs</sub>* calculation

The rates of DNA cleavage at various catalyst concentrations were determined in 20 mM HEPES, pH 7.2, at 37 °C for different intervals of time. After incubation of the pBR322 DNA and complex for a defined time, 4  $\mu$ L of loading buffer (bromophenol blue, 50% glycerol, and 2 mM EDTA) was added and stored at –20 °C. The samples were then loaded directly onto a 0.9% agarose gel and electrophoresed at a constant voltage of 70 mV for 120 min. The gels were visualized in an electrophoresis documentation and analysis system 120. Densitometric calculations were made using analysis method in Image Tools 3.00. The intensities of supercoiled pBR322 DNA were corrected by a factor of 1.42 as a result of its lower staining capacity by ethidium bromide. The decrease of form I fitted well to a single exponential decay curve. The increase of form II also fitted well to a single exponential curve, although the deviation of form II was somewhat larger than that of form I.

## Results and discussion

### Description of the molecular structures

A prospective view of complex **1** is shown in Fig. 1. Selected bond distances and angles are listed in Table 2. The structure may be contrasted with that of [Cu(bipy)<sub>2</sub>(Br)](ClO<sub>4</sub>).<sup>46</sup> It consists of a [Cu(L<sup>1</sup>)<sub>2</sub>(Br)]<sup>5+</sup> unit and five ClO<sub>4</sub><sup>–</sup> anions. The stereochemistry of the divalent Cu(1) is best described as a distorted trigonal bipyramid with the atoms N(2), N(6) and Br(1) occupying the equatorial coordination sites and N(1) and N(5) in the axial sites. The degree of distortion ( $\tau$ ) between trigonal bipyramid to square pyramid can be estimated according to Addison.<sup>47</sup> In the ideal trigonal bipyramid,  $\tau = 1$ , and in the ideal square pyramid,  $\tau = 0$ . The calculated  $\tau$  value of 0.98 indicates that

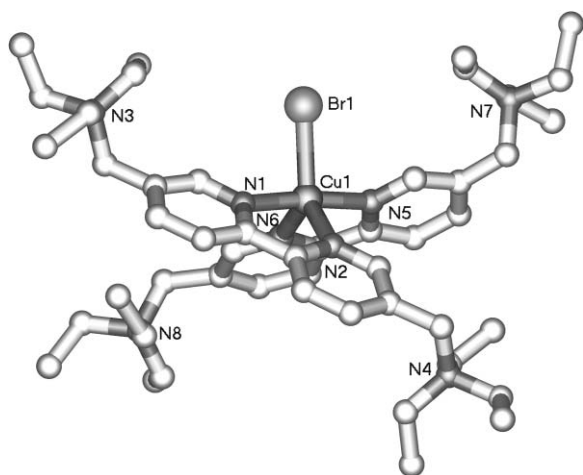


**Fig. 1** X-Ray crystal structure of **1**. Hydrogen atoms and perchlorate anions are omitted for clarity.

the geometry of coordination around the copper atom is very close to a trigonal bipyramid. The Cu(1)–Br(1) bond distance is 2.4592(6) Å, similar to copper(II) complexes with coordinated halogeno groups.<sup>46</sup> The two individual pyridine rings are coplanar. Interestingly, the two quaternary ammonium groups defined by N(3) and N(7) and the coordinated Br atom basically array in a straight line. The distances of N(3)–Br(1) and N(7)–Br(1) are 5.772 and 5.595 Å, respectively. This distance is comparable to that of adjacent phosphodiester in B-form DNA (*ca.* 6 Å).

As shown in Fig. 2, the structure of complex **2** is quite similar to **1**, except for the bulky group on each quaternary ammonium. In a similar manner to above, the calculated  $\tau$  value of 0.97 indicates that the geometry of coordination around the copper atom is also very close to a trigonal bipyramid. Selected bond distances and angles are listed in Table 3.

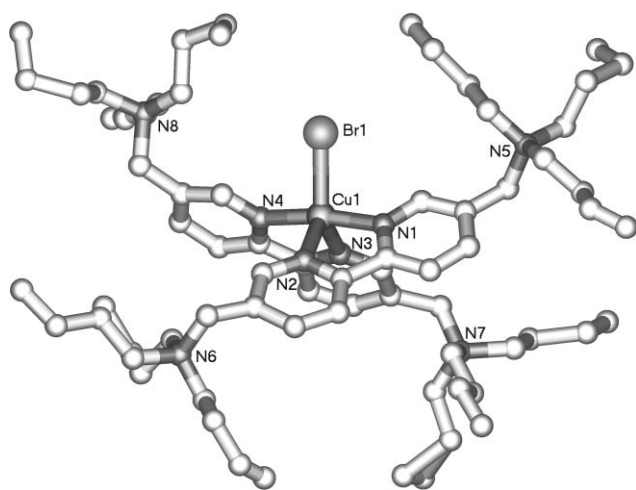


**Fig. 2** X-Ray crystal structure of **2**. Hydrogen atoms and perchlorate anions are omitted for clarity.

### DNA affinity

The interaction of the two Cu(II) complexes and [Cu(bipy)(NO<sub>3</sub>)<sub>2</sub>] with calf thymus (CT) DNA are characterized by measuring their effects on the melting temperature of DNA (Table 4). The resulting

**Table 4** Interaction of complexes with CT DNA<sup>a</sup>

Complex	$r^b$	$\Delta T_m^c/^\circ\text{C}$
<b>1</b>	0.1	3.97
	0.2	8.05
<b>2</b>	0.1	1.058
	0.2	1.461
[Cu(bipy)(NO <sub>3</sub> ) <sub>2</sub> ]	0.1	0.48
	0.2	0.55

<sup>a</sup> Reaction conditions: 20 mM HEPES at pH 8.0,  $I = 0.1$  M, [DNA] = 100  $\mu\text{M}$ . <sup>b</sup>  $r$  = Molar ratio of complex/nucleic acid phosphate, <sup>c</sup>  $\Delta T_m$  = The melting temperature of DNA with complex minus the melting temperature of DNA in the absence of complex.

$T_m$  curves are shown in Fig. 3S (ESI†). A considerable increase in the melting temperature in each case is observed, indicative of stabilization of the double-stranded nucleic acids by the metal complexes. A slightly larger stabilization effect of complex **1** than **2** is observed (Table 4).

In general, there are three interaction modes between metal complexes and DNA: electrostatic interaction, hydrophobic binding and intercalation. Both **1** and **2** show higher affinity towards CT DNA than [Cu(bipy)(NO<sub>3</sub>)<sub>2</sub>], which suggests that quaternary ammonium pendants in **1** and **2** can indeed electrostatically interact with the negatively charged phosphate backbone. Interestingly, **1** exhibits a markedly higher affinity towards DNA than **2** although they have the same charges. This indicates that larger butyl groups in **2** are less efficient toward DNA binding *via* hydrophobic binding. In contrast, the electrostatic interaction in **2** between the pendant and DNA is weaker than that of **1** due to steric hindrance. Thus, complexes with **L**<sup>1</sup> investigated are promising agents to interact with double-stranded DNA.

### DNA cleavage

The supercoiled plasmid DNA cleavage by these Cu(II) complexes and their analogues was studied in the absence of H<sub>2</sub>O<sub>2</sub> or any reducing agents (Fig. 3) and a time-dependent cleavage was

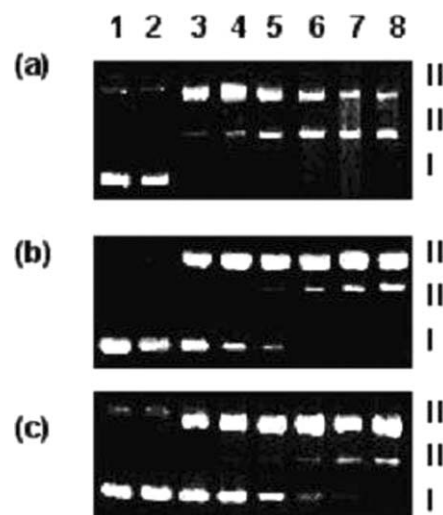


**Fig. 3** Agarose gel electrophoresis of 38  $\mu\text{M}$  pBR322 plasmid DNA at 37  $^\circ\text{C}$  in 20 mM HEPES at pH 7.2 in the presence of 150  $\mu\text{M}$  complex **1** (a), **2** (b) and [Cu(bipy)(NO<sub>3</sub>)<sub>2</sub>] (c). Lane 1: DNA control, lanes 2–8: DNA + complex for 0, 1, 2, 4, 8, 16, 24 h.

observed. The supercoiled DNA (form I) was completely cleaved by **1**, **2** and  $[\text{Cu}(\text{bipy})(\text{NO}_3)_2]$  after 1, 4 and 8 h, respectively, and the linear DNA (form III) appears up at 2, 8 and 8 h, respectively. The hydrolytic activity of **1** is much higher than the other two complexes.

In order to further clarify the DNA cleavage mechanism, complex **1** was investigated in the presence of a chelating agent (EDTA), hydroxyl radical scavengers (DMSO and *t*BuOH)<sup>48</sup> and a superoxide scavenger (SOD).<sup>49</sup> As shown in Fig. 4, EDTA can efficiently inhibit the complex activity similarly to that for nuclease. However, both DMSO and *t*BuOH are completely ineffective. This result rules out the possibility of DNA cleavage by hydroxyl radicals. When one looks closely at the data presented in Fig. 4, the addition of SOD in lane 6 caused a marked increase in strand scission. This seems to imply a role for  $\text{H}_2\text{O}_2$  in the cleavage chemistry. Therefore, the cleavage was investigated further in the presence of the enzyme catalase, which can lower solution concentrations of  $\text{H}_2\text{O}_2$  (Fig. 4S, ESI†). The result indicates that catalase does not inhibit DNA cleavage, and thus the mechanism of cleavage is not an oxidative process arising from  $\text{O}_2^-$  and  $\text{H}_2\text{O}_2$ . In the absence of any reducing agents, therefore, DNA cleavage by the **1** is likely to proceed *via* a hydrolytic degradative pathway.

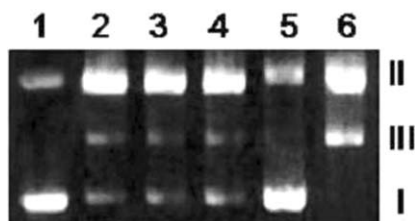


**Fig. 4** Agarose gel showing cleavage of  $38 \mu\text{M}$  pBR322 DNA incubated with **1** ( $150 \mu\text{M}$ ) in  $20 \text{ mM}$  HEPES,  $\text{pH } 7.2$  at  $37^\circ\text{C}$  for 1 h. Lane 1: DNA control, lane 2: DNA + **1**, lanes 3–6: DNA + **1** + 1 M DMSO, 1 M *t*BuOH, 0.1 M EDTA,  $1000 \text{ U mL}^{-1}$  SOD.

#### Pseudo-Michaelis–Menten kinetics of DNA cleavage

A series of typical patterns of supercoiled plasmid DNA cleavage into nicked and linear DNA by complexes **1**, **2** and  $[\text{Cu}(\text{bipy})(\text{NO}_3)_2]$  were performed under hydrolytic conditions. The disappearance of form I *vs.* time followed pseudo-first-order kinetic profiles and can be well fitted by a single exponential function (Fig. 5S, ESI†). Further, saturation kinetics of DNA cleavage were studied using various concentrations of complexes ( $30$ – $210 \mu\text{M}$ ). The pseudo-Michaelis–Menten kinetic parameters ( $k_{\text{cat}}$  and  $K_{\text{M}}$ ) were calculated to be  $4.15 \text{ h}^{-1}$  and  $6.5 \times 10^{-5} \text{ M}$  for **1**,  $0.43 \text{ h}^{-1}$  and  $7.5 \times 10^{-5} \text{ M}$  for **2**, and  $0.61 \text{ h}^{-1}$  and  $3.3 \times 10^{-4} \text{ M}$  for  $[\text{Cu}(\text{bipy})(\text{NO}_3)_2]$ , respectively, based on plots of  $k_{\text{obs}}$  *vs.* concentration of the complex, Fig. 5.

The obtained hydrolysis rate constants show that **1** has a very high nuclease activity, giving  $1.2 \times 10^8$  fold rate enhancement over unhydrolyzed double-stranded DNA. Many rate constants of DNA cleavage hydrolyzed by  $\text{Cu}(\text{II})$  complexes have been reported;<sup>12a,16b,19,22</sup> the rates of hydrolysis of form I are generally in the range of  $10^{-2}$ – $1.0 \text{ h}^{-1}$ .<sup>19</sup> Only three mononuclear complexes exhibited very high nuclease activities: a  $\text{Cu}$ –dpq complex with a rate constant of  $5.58 \text{ h}^{-1}$  at  $\text{pH} = 7.2$ ,<sup>12a</sup> a  $\text{Cu}$ –tach complex with a rate constant of  $4.34 \text{ h}^{-1}$  at  $\text{pH} = 8.1$ <sup>22</sup> and a  $\text{Cu}$ –neamin complex with a rate constant of  $3.57 \text{ h}^{-1}$  at  $\text{pH} = 7.3$ .<sup>19</sup>

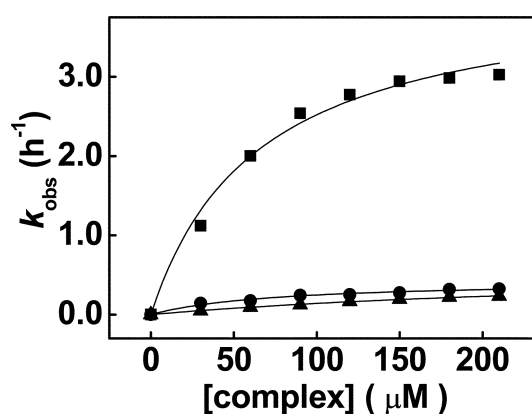


**Fig. 5** Kinetics for the cleavage of plasmid pBR322 DNA by **1** (■), **2** (●) and  $[\text{Cu}(\text{bipy})(\text{NO}_3)_2]$  (▲) in  $20 \text{ mM}$  HEPES,  $\text{pH } 7.2$  at  $37^\circ\text{C}$ . The samples were run on a  $0.9\%$  agarose gel and stained with ethidium bromide.

Unexpectedly, the DNA cleavage activity of complex **1** is about 10-fold higher than its two analogues, complex **2** and  $\text{Cu}(\text{bipy})(\text{NO}_3)_2$ . In the absence of  $\text{Cu}(\text{II})$  ion, neither  $\text{L}^1$  nor  $\text{L}^2$ , has nuclease activity, which confirms that the two triethyl quaternary ammonium pendants in **1** facilitate binding of the  $\text{Cu}^{\text{II}}$ –bipy moiety to DNA and subsequently accelerates DNA cleavage. It has been widely accepted that the metal-bound hydroxyl species ( $\text{LM-OH}$ ) in enzymes or their models are the active species in the hydration of the phosphate backbone. In aqueous solution, the  $\text{Cu-Br}$  bond in  $[\text{Cu}(\text{L})_2(\text{Br})]^{5+}$  ion is highly labile and the  $\text{Br}^-$  anion exchanges readily with a water molecule to give a  $[\text{Cu}(\text{L})_2(\text{H}_2\text{O})]^{6+}$  ion, and further leads to the formation of the active species  $[\text{Cu}(\text{L})_2(\text{OH})]^{5+}$  *via* deprotonation of the bound water molecule. The distances between coordinated hydroxyl anion and quaternary ammonium ion are around  $5.5$ – $5.7 \text{ \AA}$  in **1**, similar to the distance between adjacent phosphorus atoms of the phosphodiester in a DNA backbone (*ca.*  $6 \text{ \AA}$ ). This suggests that the three sites in **1** can synchronously interact with three phosphodiester groups in a DNA strand, Fig. 6. The direct interaction between the neighboring phosphoryl oxygen atoms and quaternary ammonium ions facilitates the formation of an intermediate, which allows the DNA to be cleaved readily.

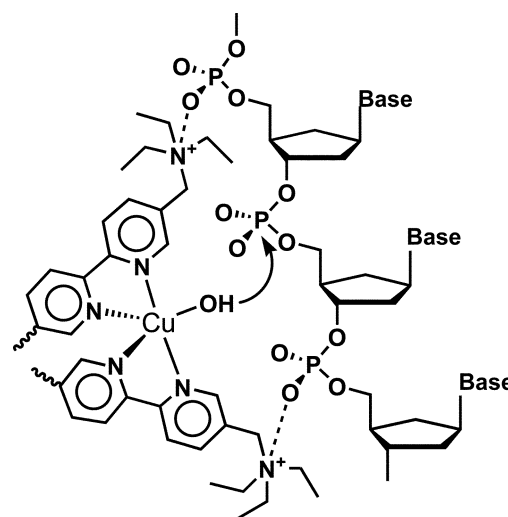


**Fig. 6** The proposed intermediate of DNA cleavage by **1**.

Therefore, the higher activity of **1** can be attributed to its special structure matching with the phosphodiester backbone of nucleic acid and cooperative interaction from the highly active (bipy)<sub>2</sub>Cu<sup>II</sup>-H<sub>2</sub>O moiety and two positive pendants. For complex **2**, the large butyl groups probably prevent nucleophilic attack of the (bipy)<sub>2</sub>Cu<sup>II</sup>-OH moiety to phosphodiester and therefore results in its lower nuclease activity.

## Conclusion

Although complexes **1** and **2** have similar Cu(II) structural configurations, **1** exhibits higher nuclease activity and give *ca.* 10-fold rate acceleration for hydrolyzing the phosphate diesters relative to **2** and its unmodified analogue. The unique acceleration could be attributed to the presence of the two positive pendants. If pendants have too large steric groups, however, the hydrolysis rate constants of DNA cleavage not only cannot increase but also markedly decrease. What is clearly of significance is that these models structurally match with the phosphodiester backbone of nucleic acid.

## Acknowledgements

This work was supported by the National Natural Science Foundation of China (Grant No: 20231010, 20529101), Ministry of Education of China and the Guangdong provincial Natural Science Foundation (04009703). We are especially thankful to Prof. Hongzhe Sun (Hong Kong University) for valuable discussions and Prof. Xiao-Ming Chen for providing access to low-temperature CCD equipment.

## References

- 1 J. Suh, *Acc. Chem. Res.*, 2003, **36**, 562.
- 2 (a) A. Sreedhara and J. A. Cowan, *J. Biol. Inorg. Chem.*, 2001, **6**, 337; (b) J. A. Cowan, *Chem. Rev.*, 1998, **98**, 1067.
- 3 N. H. Williams, B. Takasaki, M. Wall and J. Chin, *Acc. Chem. Res.*, 1999, **32**, 485.
- 4 E. L. Hegg and J. N. Burstyn, *Coord. Chem. Rev.*, 1998, **173**, 133.
- 5 C. J. Burrows and J. G. Muller, *Chem. Rev.*, 1998, **98**, 1109.
- 6 W. K. Pogozelski and T. D. Tullius, *Chem. Rev.*, 1998, **98**, 1089.
- 7 R. R. Breaker, *Chem. Rev.*, 1997, **97**, 371.
- 8 D. E. Wilcox, *Chem. Rev.*, 1996, **96**, 2435.
- 9 D. S. Sigman, A. Mazumder and D. M. Perrin, *Chem. Rev.*, 1993, **93**, 2295.
- 10 D. S. Sigman, *Acc. Chem. Res.*, 1986, **19**, 180.
- 11 (a) J. R. Morrow and W. C. Trogler, *Inorg. Chem.*, 1988, **27**, 3387; (b) J. R. Morrow, L. A. Buttrey and K. A. Berback, *Inorg. Chem.*, 1992, **31**, 16.
- 12 (a) S. Dhar, P. A. N. Reddy and A. R. Chakravarty, *Dalton Trans.*, 2004, 697; (b) P. A. N. Reddy, M. Nethaji and A. R. Chakravarty, *Eur. J. Inorg. Chem.*, 2004, 1440.
- 13 X. M. Xu, J. H. Yao, Z. W. Mao, K. B. Yu and L. N. Ji, *Inorg. Chem. Commun.*, 2004, **7**, 803.
- 14 (a) L. P. Lu, M. L. Zhu and P. Yang, *J. Inorg. Biochem.*, 2003, **95**, 31; (b) R. Ren, P. Yang, W. J. Zheng and Z. C. Hua, *Inorg. Chem.*, 2000, **39**, 5454.
- 15 A. M. Thomas, M. Nethaji, S. Mahadevan and A. R. Chakravarty, *J. Inorg. Biochem.*, 2003, **94**, 171.
- 16 (a) M. Kathryn, T. Deck, A. Tseng and J. N. Burstyn, *Inorg. Chem.*, 2002, **41**, 669; (b) E. L. Hegg and J. N. Burstyn, *Inorg. Chem.*, 1996, **35**, 7474.
- 17 J. Gao, A. E. Martell and J. Reibenspies, *Inorg. Chim. Acta*, 2002, **329**, 122.
- 18 M. Jezowska-Bojczuk, W. Lesniak, W. Szczepanik, K. Gatner, A. Jezierski, M. Smoluch and W. Bal, *J. Inorg. Biochem.*, 2001, **84**, 189.
- 19 A. Sreedhara, J. D. Freed and J. A. Cowan, *J. Am. Chem. Soc.*, 2000, **122**, 8814.
- 20 (a) D. K. Chand, H. J. Schneider, A. Bencini, A. Bianchi, C. Giorgi, S. Ciattini and B. Valtancoli, *Chem.–Eur. J.*, 2000, **6**, 4001; (b) D. K. Chand, H. J. Schneider, J. A. Aguilar, F. Escarti, E. Garcia-Espan and S. V. Luis, *Inorg. Chim. Acta*, 2000, **316**, 71.
- 21 (a) M. S. Melvin, J. T. Tomlinson, G. R. Saluta, G. L. Kucera, N. Lindquist and R. A. Manderville, *J. Am. Chem. Soc.*, 2000, **122**, 6333; (b) S. Borah, M. S. Melvin, N. Lindquist and R. A. Manderville, *J. Am. Chem. Soc.*, 1998, **120**, 4557.
- 22 U. Itoh, H. Hisada, T. Sumiya, M. Hosono, Y. Usui and Y. Fujii, *Chem. Commun.*, 1997, 677.
- 23 (a) F. V. Pamatong, C. A. Detmer, III and J. R. Bocarsly, *J. Am. Chem. Soc.*, 1996, **118**, 5339; (b) C. A. Detmer, III, F. V. Pamatong and J. R. Bocarsly, *Inorg. Chem.*, 1996, **35**, 6292.
- 24 S. C. Zhang, Y. Shao, C. Tu, C. H. Dai and Z. J. Guo, *Chin. J. Inorg. Chem.*, 2004, **20**, 1159.
- 25 M. Gonzalez-Alvarez, G. Alzuet, J. Borrás, M. Pitie and B. Meunier, *J. Biol. Inorg. Chem.*, 2003, **8**, 644.
- 26 L. P. Lu, M. L. Zhu and P. Yang, *J. Inorg. Biochem.*, 2003, **95**, 31.
- 27 D. Y. Kong, J. Reibenspies, J. G. Mao, A. Clearfield and A. E. Martell, *Inorg. Chim. Acta*, 2003, **342**, 158.
- 28 L. Zhu, U. dos Santos, C. W. Koo, M. Rybstein, L. Pape and J. W. Canary, *Inorg. Chem.*, 2003, **42**, 7912.
- 29 L. M. Rossi, A. Neves, R. Horner, H. Terenzi, B. Szpoganicz and J. Sugai, *Inorg. Chim. Acta*, 2002, **337**, 366.
- 30 A. M. Thomas, G. Neelakanta, S. Mahadevan, M. Nethaji and A. R. Chakravarty, *Eur. J. Inorg. Chem.*, 2002, 2720.
- 31 (a) K. J. Humphreys, K. D. Karlin and S. E. Rokita, *J. Am. Chem. Soc.*, 2002, **124**, 6009; (b) K. J. Humphreys, A. E. Johnson, K. D. Karlin and S. E. Rokita, *J. Biol. Inorg. Chem.*, 2002, **7**, 835.
- 32 G. N. De Iulius, G. A. Lawrance and S. Fieuw-Makaroff, *Inorg. Chem. Commun.*, 2000, **3**, 307.
- 33 C. Tu, Y. Shao, N. Gan, D. Xu and Z. J. Guo, *Inorg. Chem.*, 2004, **43**, 4761.
- 34 A. Bencini, E. Berni, A. Bianchi, C. Giorgi, B. Valtancoli, D. K. Chand and H. J. Schneider, *Dalton Trans.*, 2003, 793.
- 35 K. J. Humphreys, K. D. Karlin and S. E. Rokita, *J. Am. Chem. Soc.*, 2002, **124**, 8055.
- 36 I. O. Fritsky, R. Ott, H. Pritzkow and R. Kramer, *Chem.–Eur. J.*, 2001, **7**, 1221.
- 37 P. Molenveld, J. F. J. Engbersen and D. N. Reinhoudt, *Angew. Chem., Int. Ed.*, 1999, **38**, 3189.
- 38 S. G. Srivatsan and S. Verma, *Chem.–Eur. J.*, 2001, **7**, 828.
- 39 (a) J. Suh and S. J. Moon, *Inorg. Chem.*, 2001, **40**, 4890; (b) B. B. Jang, K. P. Lee, D. H. Min and J. Suh, *J. Am. Chem. Soc.*, 1998, **120**, 12008.
- 40 W. N. Lipscomb and N. Strater, *Chem. Rev.*, 1996, **96**, 2375.
- 41 E. Kovari, J. Heitker and R. Kramer, *J. Chem. Soc., Chem. Commun.*, 1995, 1205.
- 42 R. Hettich and H. J. Schneider, *J. Am. Chem. Soc.*, 1997, **119**, 5638.
- 43 G. M. Sheldrick, *SADABS 2.05*, University of Göttingen, 2002.
- 44 *SHELXTL 6.10*, Bruker Analytical Instrumentation, Madison, WI, USA, 2000.
- 45 L. E. Gunther and A. S. Yong, *J. Am. Chem. Soc.*, 1968, **90**, 7323.
- 46 C. O'Sullivan, G. Murphy, B. Murphy and B. Hathaway, *J. Chem. Soc., Dalton Trans.*, 1999, 1835.
- 47 A. W. Addison and T. N. Rao, *J. Chem. Soc., Dalton Trans.*, 1984, 1349.
- 48 O. I. Aruoma, B. Halliwell and M. Dizdaroglu, *J. Biol. Chem.*, 1989, **264**, 13024.
- 49 K. Yamamoto and S. Kawanishi, *J. Biol. Chem.*, 1989, **264**, 15435.